FERRIC/FERROUS DETERMINATIONS IN SYNTHETIC BIOTITE

by

Elizabeth Partin

Thesis submitted to the Faculty of the

Virginia Polytechnic Institute and State University

in partial fulfillment of the requirements for the degree of

MASTER OF SCIENCE

IN

GEOLOGICAL SCIENCES

APPROVED:

David A. Hewitt, Chairman	David R. Wones
J. Donald Rimstidt	Paul H. Ribbe

January 9, 1984

Blacksburg, Virginia

FERRIC/FERROUS DETERMINATIONS IN SYNTHETIC BIOTITE

by

Elizabeth Partin

(ABSTRACT)

The relationships between ferric iron content and the P-T-fH_2 conditions of formation were examined for two biotite compositions: annite ($K_2Fe_5Al_4Si_5O_{20}(OH)_4$) and siderophyllite ($K_2Fe_6Al_2Si_6O_{20}(OH)_4$). The synthesized phases were annealed at fixed hydrogen fugacities using both the solid oxygen buffering technique of Eugster (1957) and the H_2 buffering technique of Shaw (1967). Resulting hydrogen fugacities ranged from 0.004 bars (at T = 400°C, P_T = 2 kb) to 51 bars (at T = 750°C, P_T = 1 kb).

Ferrous iron contents of the annealed biotites were determined by wet chemical analyses. Total iron was determined by microprobe analyses to be equal to the stoichiometric values. The data confirm the predictions of Hazen and Wones (1972, 1978) that: 1) There is a structural limit imposed upon the Fe^{3+} content of annite due to the misfit between the octahedral and tetrahedral layers. This misfit requires a minimum of 11% Fe^{3+} in annite. 2) The steric misfit in annite can be corrected by a substitution of $Al^{vi} + Al^{iv}$ for $Fe^{vi} + Si^{iv}$, so that

there is no Fe^{3+} in siderophyllite at high hydrogen fugacities.

A model relating Fe^{3+}/Fe^{2+} ratios, fH_2, and T is proposed. The model accounts for the amount of Fe^{3+} needed to correct the steric misfit in annite and allows for variation in Fe, Al, and Mg contents among biotites. A simple oxidation-reduction reaction is used to relate changes in the non-steric ferric iron to hydrogen fugacity and temperatures for the Fe-Mg-Al biotites. The equilibrium constant for the reaction can be expressed as: (1) $\log K = \frac{3607.2}{T} - 4.47$

where, depending on composition, K is expressed as follows and R is a constant proportional to the structurally required iron.

(2) $\frac{Al^{vi}}{0.3} + \frac{Mg}{0.72} \geq 1, \quad K = \frac{Fe^{3+}}{Fe^{2+}} fH_2^{\frac{1}{2}}$

$(Al^{vi} + Mg \geq 1)$

(3) $\frac{Al^{vi}}{0.3} + \frac{Mg}{0.72} \geq 1, \quad K = \frac{Fe^{3+}}{Fe^{2+} - (1-Al^{vi}-Mg)} fH_2^{\frac{1}{2}}$

$(Al^{vi} + Mg < 1)$

(4) $\frac{Al^{vi}}{0.3} + \frac{Mg}{0.72} < 1, \quad K = [\frac{Fe^{3+}}{Fe^{2+} - (1-Al^{vi}-Mg)} - 0.185] fH_2^{\frac{1}{2}}$

$(Al^{vi} + Mg < 1)$

ACKNOWLEDGEMENTS

I would first like to thank my parents, and , without whose steady moral and financial support I would not have been able to successfully undertake a masters program. I would also like to especially thank Dr. David A. Hewitt, whose encouragement and patience has had a great deal to do with the success of my graduate career. The support and assistance from my other commitee members, Drs. P. H. Ribbe, J. D. Rimstidt, and D. R. Wones, was also greatly appreciated. Additional financial support came from a Sigma Xi Research Grant, and was greatly appreciated. I recieved valuable analytical assistance from and technical support from , , , and , all from V. P. I. and S. U..

TABLE OF CONTENTS

LIST OF FIGURES

LIST OF TABLES

Introduction

Biotites occur in a wide variety of geologic settings. They are often present as a major phase in felsic to intermediate igneous rocks and occur widely in metamorphic rocks of a range of bulk composition at or above the greenschist facies. This nearly ubiquitous occurrence makes them useful for thermobarometry. To date, there have been two kinds of P-T indicators developed using Fe-bearing biotites. First, there are the equilibria involving the decomposition of biotite (Eugster and Wones, 1962; Wones and Eugster, 1965; Rutherford, 1969, 1973; Hewitt and Wones, 1981) and biotite plus quartz (Wones and Eugster, 1965). For rocks containing the appropriate phases, these equilibria provide a valuable relationship among temperature, pressure and oxygen fugacity. Second, there are exchange equilibria involving the distribution of elements such as Fe and Mg or OH and F among biotites and garnets, cordierites or muscovites (Ferry and Spear, 1978; Holdaway and Lee, 1977; Munoz and Ludington, 1974). The distribution coefficients for these exchange reactions have been used extensively in interpreting the P-T conditions for many metamorphic and igneous rocks.

None of the systems discussed above consider the role of ferric iron in biotite. Wones, Burns and Carroll

(1971) reported the ferric iron contents of some synthetic annites, but no systematic study of the ferric iron content of biotite as a function of pressure, temperature and oxygen fugacity has been undertaken. A knowledge of the ferric iron content in synthetic and natural biotite is essential to the application of experimental data to natural systems and may well provide an additional T-fO_2 indicator requiring only the presence of biotite and the determination of its composition.

This study was undertaken to develop a functional correlation between the ferric iron content of the Fe-Al biotites and the P-T-fH_2 conditions of their formation. The phase equilibria for the biotites in this study, annite $[K_2Fe_6Al_2Si_6O_{20}(OH)_4]$ and siderophyllite $[K_2Fe_5Al_4Si_5O_{20}(OH)_4]$, are already fairly well defined (Eugster and Wones, 1962; Wones and Eugster, 1965; Hewitt and Wones ,1975, 1981; Rutherford, 1973). These compositions were chosen because the stability data were known and because some ferric iron contents of synthetic annite had already been reported by Wones, Burns and Carroll (1971). In addition, knowing the ferric iron contents of annite and siderophyllite under similar conditions would provide a basis for an evaluation of the crystallographic arguments on biotite presented by Hazen and Wones (1972).

According to Hazen and Wones, the ferric iron content of annite is a complex variable dependent on steric details of the biotite structure as well as the oxidizing conditions of the system. Trioctahedral micas are characterized by geometrical differences between the octahedral and tetrahedral layers. For a given tetrahedral composition, the articulation between the layers is primarily controlled by the octahedral layer; specifically by the mean M-O distance, which in turn is a function of composition, pressure and temperature. The tetrahedral sheet can adjust to match a smaller octahedral sheet by rotation of the tetrahedra from a perfect hexagonal net ($\alpha = 0°$) to a trigonal one ($\alpha = 30°$). In common biotites this rotation is limited to the range $0° \leq \alpha \leq 12°$, based on the observations of Guidotti (1975). For this range of α, the ratio of the mean M-O bondlength to the mean T-O bondlength (which is constant for a given composition at any P-T) has been defined by Hazen and Wones (1972, 1978) to be; $1.235 \leq d_o/d_t \leq 1.275$ Å. These restrictions show that the pure endmember annite is geometrically unstable with $d_o/d_t = 1.285$ Å at $\alpha = 0°$. Hazen and Wones give four possible ways of stabilizing the annite; the two reactions given below pertain to this study.

(1) $^{vi}R^{2+} + (OH)^- = {}^{vi}R^{3+} + O^=$ and

(2) $^{iv}Al^{3+} + {}^{vi}Al^{3+} = {}^{iv}Si^{4+} + {}^{vi}R^{2+}$

Oxidation of about 10% of the ferrous iron in annite according to reaction (1) gives a d_o value of 2.105 Å and ratio of 1.275, just within the proposed limits. Any change in the oxidation state of iron beyond the initial 10-11% would then be a function of the oxygen fugacity of the environment.

Reaction (2), the substitution leading toward siderophyllite, has the effect of reducing the size of the octahedral layer (Al^{3+} for Fe^{2+}) and increasing the size of the tetrahedral layer (Al^{3+} for Si^{4+}), thereby stabilizing the structure. Obviously, given a sufficient amount of this substitution, there should be no structural need for ferric iron in siderophyllite.

Experimental Methods

Biotites were synthesized from oxide mixes containing reagent grade Fe_2O_3, $K_2Si_4O_9$ (n = 1.493) or $K_2Si_6O_{13}$ (n = 1.492) glass (produced according to the method of Schairer and Bowen (1955)), SiO_2 glass (Corning Lump Cullet #7940) and γ-Al_2O_3 produced by firing $AlCl_3 \cdot 6H_2O$. Oxides were mixed according to the appropriate stoichiometries and ground under acetone or alcohol until

they were optically homogeneous. The mixes were then reduced in a hydrogen atmosphere at approximately 500°C.

Syntheses were carried out using standard hydrothermal techniques, in Tuttle cold-seal Rene 41 bombs (Tuttle, 1949). The charges were packed into $Ag_{70}Pd_{30}$ capsules with excess distilled water and were equilibrated at temperatures between 550 and 670°C and pressures of 2 or 4 kbars. Run times ranged from 3 to 13 days. Temperatures were measured with chromel-alumel thermocouples that were calibrated against the melting points of NaCl, KCl, and CsCl and are considered to be accurate to within ±5°C. Pressures were measured with a Harwood Manganin Cell calibrated against a Heise gauge and are thought to be accurate to within ±50 bars.

Runs yielding ≥98% biotite by optical and X-ray examination were reground under acetone or alcohol and annealed. Some biotites were rerun in a hydrogen diffusion system (Shaw, 1967; Hewitt, 1977) at hydrogen pressures of 5, 25, and 50 bars. Run temperatures were chosen as close to the maximum thermal stability as practical. The equilibria data from Hewitt and Wones (1981) and Rutherford (1973) on annite and siderophyllite, respectively, were used as guides to the thermal stability. Pressures for runs in the Shaw bombs were measured with Heise gauges, and are accurate to ±10

bars for the total pressure (1 kbar) and about ±0.1 bar for the hydrogen pressures. Other biotites were rerun using the solid oxygen buffering technique of Eugster (1957). The fayalite-magnetite-quartz (FMQ) equilibrium of Hewitt (1978), the nickel-nickel oxide (NNO) equilibrium of Huebner and Sato (1970), and the magnetite-hematite (MH) equilibrium of Myers and Eugster (1983) were used to calculate fO_2 values. Temperatures for these annealing experiments were also chosen near the maximum thermal stability. Table 1 is a compilation of the run data.

The biotites from the annealing experiments ranged in size from 1 micron to 15-20 microns in the longest dimension. Annites were consistently larger than siderophyllites; while the annites ranged up to 20 microns, the siderophyllites only grew to about 1-2 microns. SEM photos (figure 1, a and b) show the euhedral platy nature of both micas. The edges of the grains are clean and there are no signs of dissolution. These equilibrium crystal forms suggest that there was no anomalous contribution of surface free energy by the reacting grains.

Table 1. Run data for all synthetic annites and siderophyllites, with $Fe^{2+}/ Fe^{2+} + Fe^{3+}$ ratios.

Run Number	X	P_{H_2}	P_T	T	No. Days	$\frac{Fe^{2+}}{Fe^{2+}+Fe^{3+}}$
A34*	ann	101.6	1	791	-	0.894
182	ann	51.9	1	750	8	0.889
282	ann	51.9	1	750	8	0.887
7a82	ann	51.9	1	750	5	0.895
8-80**	ann	51.9	1	750	7	0.886
14a83	ann	26.1	1	710	4	0.897
14b/15a	ann	26.1	1	700	5	0.844
9a82	ann	26.1	1	700	6	n.d.
3483	ann	10.4	2	670	5	0.759
A50*	ann	10.0	1	635	-	0.837
A21*	ann	10.0	1	606	-	0.805
15a82	ann	6.0	1	615	6	0.822
14a82	ann	6.0	1	615	9	0.814
11a82	ann	6.0	1	615	9	0.811
12a82	ann	6.0	1	615	9	0.810
2383	ann	4.0	2	600	8	0.769
1083	ann	4.0	2	600	9	n.d.
A30*	ann	0.004	2	399	-	0.718
3283	sdp	51.9	1	750	4	1.003
3083	sdp	26.1	1	700	4	0.983
21a83	sdp	26.1	1	700	3	0.959
2483	sdp	10.4	2	670	7	0.880
3183	sdp	6.0	1	615	3	0.932
11a83	sdp	6.0	1	615	7	0.886
2583	sdp	4.0	2	600	6	0.856
1783	sdp	0.004	2	400	13	0.789

* Wones, personal communication
** Hewitt, personal communication

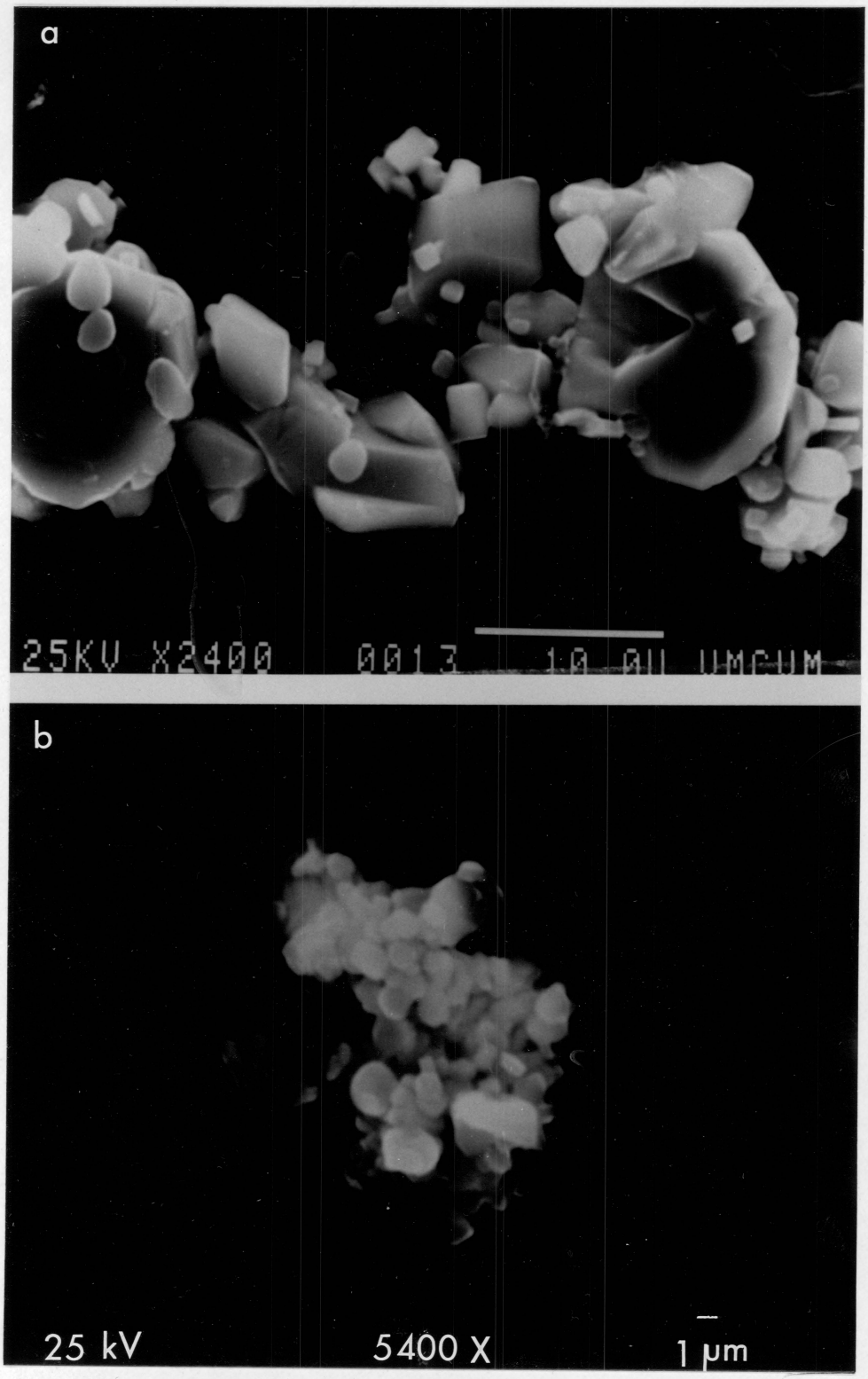

Figure 1a. SEM photomicrograph of annite 3483, annealed on the FMQ buffer. b. SEM photomicrograph of siderophyllite 3283, annealed at 51 bars P_{H_2}.

Analytical Methods and Experimental Results

Unit cell dimensions were obtained by x-ray powder diffraction methods using an automated Phillips x-ray diffractometer with CuKα radiation and CaF_2 as an internal standard. Peak data were refined using the LSUCR program of Appleman and Evans (1973), assuming a 1M polytype (C2/m). Results are listed in table 2 and plots of unit cell parameters versus composition are shown in figures 2 through 4.

Plots of d_{001} and unit cell volume versus composition (figures 3 and 4) show linear trends for both annite and siderophyllite, indicating the possibility of using these parameters as indicators of the compositions of Fe-rich biotites, although the accuracy is only ±0.05 mole fraction Fe^{2+}. Extrapolation of the volume plot (figure 4) to the compositions for ideal annite and ideal oxyannite yields molar volumes for these phases of 155.5 and 150.9 cm^3mol^{-1}, respectively.

The siderophyllite cell volumes (especially the 50 bar point) compare favorably with those obtained by Hewitt and Wones (1975); their run at 100 bars H_2 yielded a volume of 506.7 $Å^3$. This suggests that siderophyllite has reached its maximum expansion at 50 bars H_2 and also suggests that the maximum amount of reduced iron is incorporated into the structure at 50 bars H_2.

Table 2. Unit cell parameters and γ-refractive index measurements for selected samples. Refinements were calculated using at least 10 distinct peaks.

	Run No.	a(Å)	b(Å)	c(Å)	β	V(Å^3)	γ-R.I.	$\frac{Fe^{2+}}{Fe^{2+}+Fe^{3+}}$
annite	A34[2]	5.398(1)[1]	9.349(3)	10.330(3)	100°4'(1)	513.4(2)	1.689(3)	.894
	7a82	5.399(2)	9.359(3)	10.339(3)	100°9'(2)	514.3(2)	1.692(1)	.895
	9a82[3]	5.398(2)	9.341(5)	10.336(5)	100°4'(3)	513.1(3)	1.690(2)	.844
	3483	5.393(2)	9.340(2)	10.300(4)	100°5'(2)	510.8(2)	1.694(2)	.759
	15a83	5.395(1)	9.342(2)	10.309(1)	100°5'(1)	511.1(1)	1.692(2)	.822
	1083[4]	5.398(3)	9.341(8)	10.319(6)	100°8'(4)	512.2(5)	1.699(1)	.769
	A30[2]	5.397(4)	9.324(2)	10.272(5)	99°55'(3)	509.2(4)	1.698	.718
siderophyllite	3283	5.373(9)	9.315(3)	10.277(4)	100°1'(4)	506.4(8)	1.675(2)	1.00
	3083	5.374(7)	9.309(2)	10.269(5)	100°2'(3)	505.9(6)	1.675(2)	.983
	2483	5.358(5)	9.298(2)	10.253(3)	100°2'(2)	502.9(4)	n.d.	.880
	11a83	5.371(2)	9.301(2)	10.269(2)	100°5'(2)	505.1(2)	1.677(2)	.886
	2583	5.372(4)	9.274(2)	10.249(3)	100°2'(2)	502.8(3)	1.680(2)	.856
	1783	5.367(5)	9.282(2)	10.251(3)	100°5'(3)	502.7(5)	1.678(2)	.789

1 Numbers in parentheses indicate uncertainty in the digit immediately to the left
2 Wones, personal communication
3 Titration data from 14b/15a83 (same run conditions)
4 Titration data from 2383 (same run conditions)

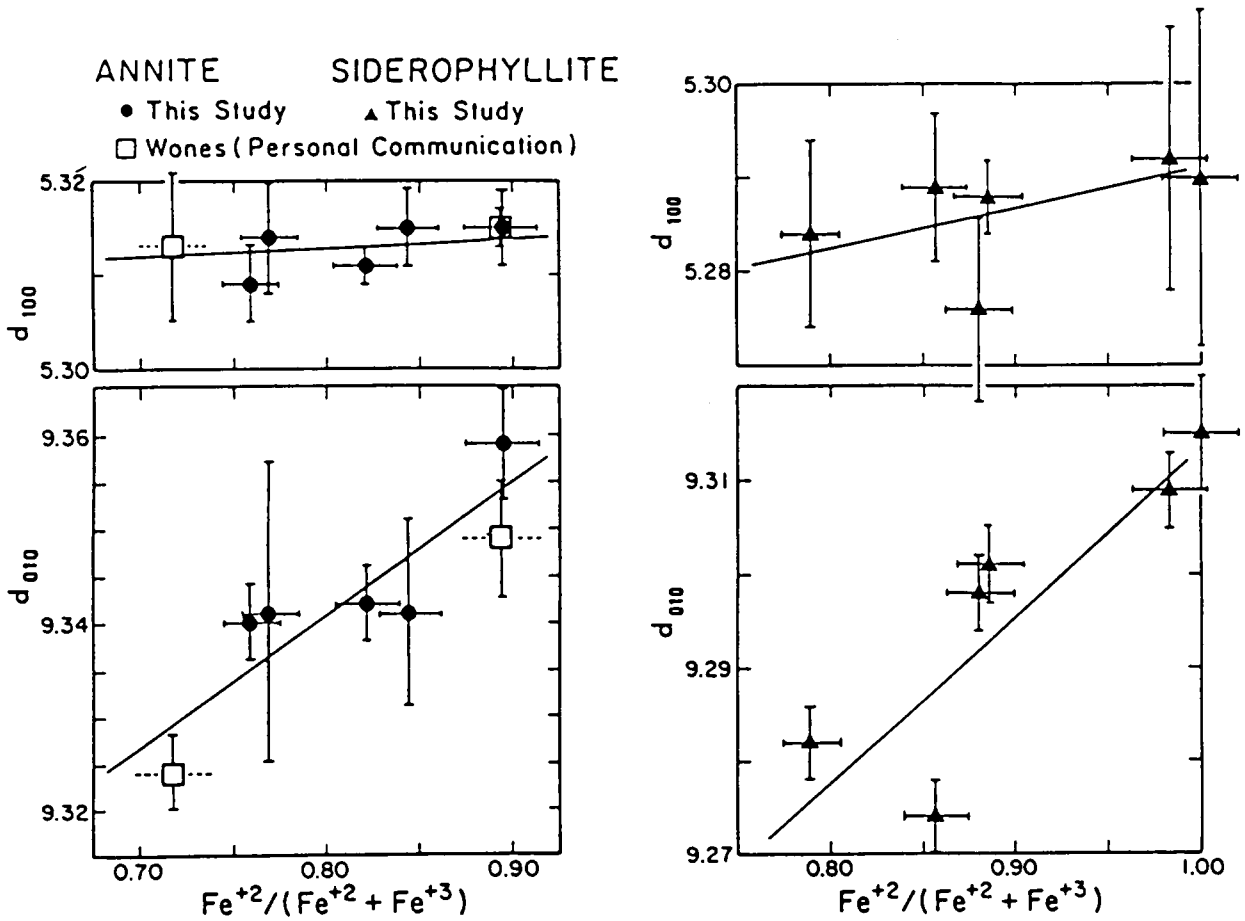

Figure 2. d_{100} and d_{010} versus $Fe^{2+}/ Fe^{2+} + Fe^{3+}$ ratios for selected annites and siderophyllites, listed in Table 2. Vertical error bars represent 2σ standard deviations in the cell dimension; horizontal error bars represent the analytical error in the iron ratios.

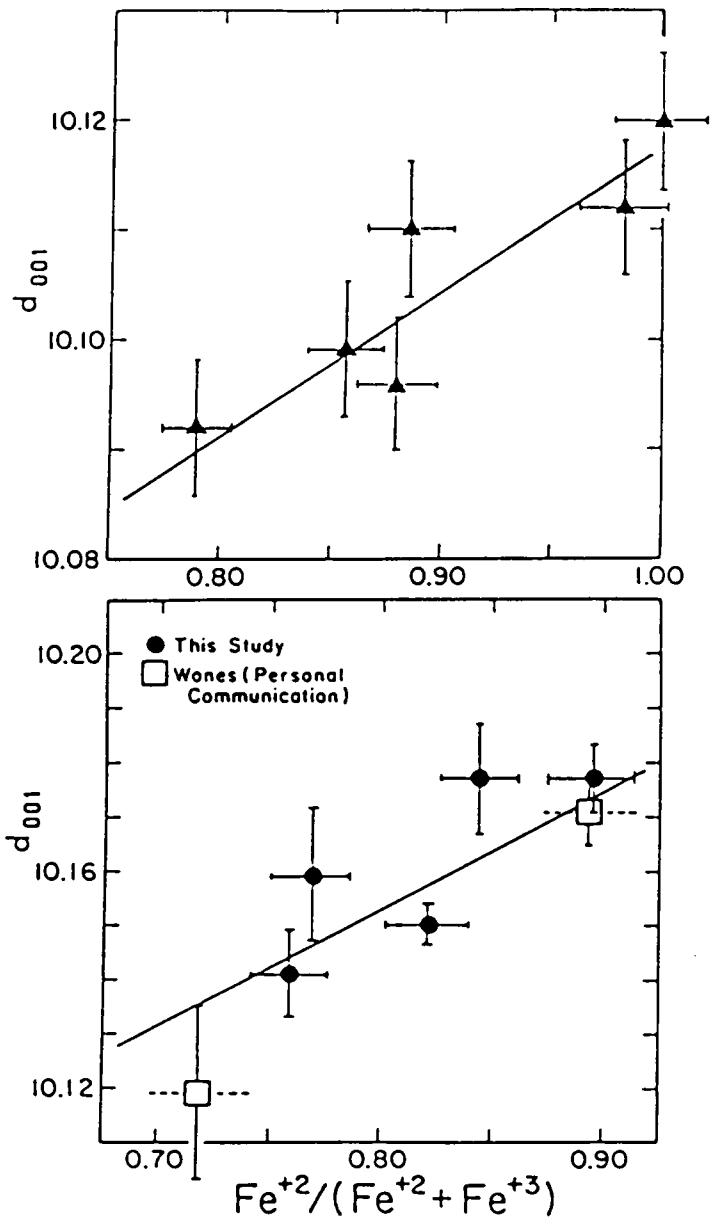

Figure 3. d_{001} versus $Fe^{2+}/Fe^{2+}+Fe^{3+}$ ratios for biotites listed in Table 2. Errors are as in figure 2.

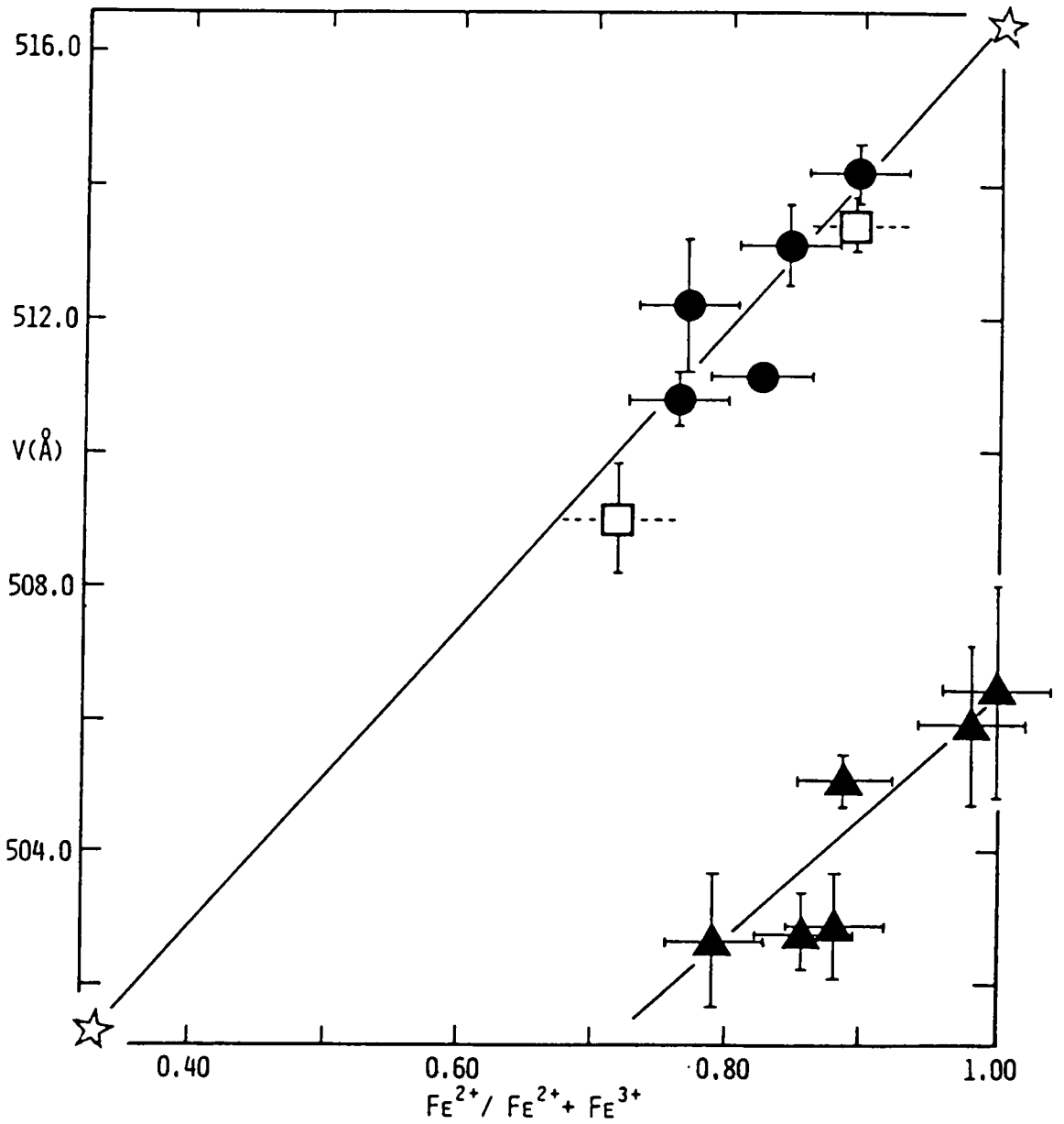

Figure 4. Unit cell volumes versus $Fe^{2+}/Fe^{2+}+Fe^{3+}$ ratios for biotites listed in Table 2. Extrapolation of annite line is to pure ideal annite at 100 % ferrous iron and to pure ideal oxyannite at 33 % ferrous iron. Errors are as in previous figures.

Annites are green in color with increasing olive-green to dark red-brown pleochroism as Fe^{3+} content increases. Good "bird's eye" extinction can be seen in some larger crystals. Siderophyllites are bluish green and the color becomes slightly more intense as Fe^{3+} increases. Pleochroism and color are difficult to see in the siderophyllites because the crystals are very fine grained.

Temperature-corrected γ refractive indices were measured at 25°C under sodium light using calibrated Cargille oils. These are plotted against the ferrous to total iron ratios in figure 5. These curves may be used as composition indicators for Fe-rich biotites to within ±0.05 mole fraction ferrous iron.

The compositions and stoichiometries of the biotites were determined by microprobe analyses, using a 9-spectrometer ARL-SEMQ electron microprobe, run at 10 kV accelerating voltage with a sample current of 10 nA. A natural fayalite from Rockport, Mass. (FeO = 66.5 wt %) and an orthoclase from Benson Mines, N.Y. ($Or_{92}Ab_8$) were used as standards for Fe and K, Al, Si, respectively. Analyses commonly summed to significantly less than the ideal 96% for hydrous biotite because of the fine grained nature of the biotites (≤20 microns). Final compositions were taken as extrapolated values according to the method

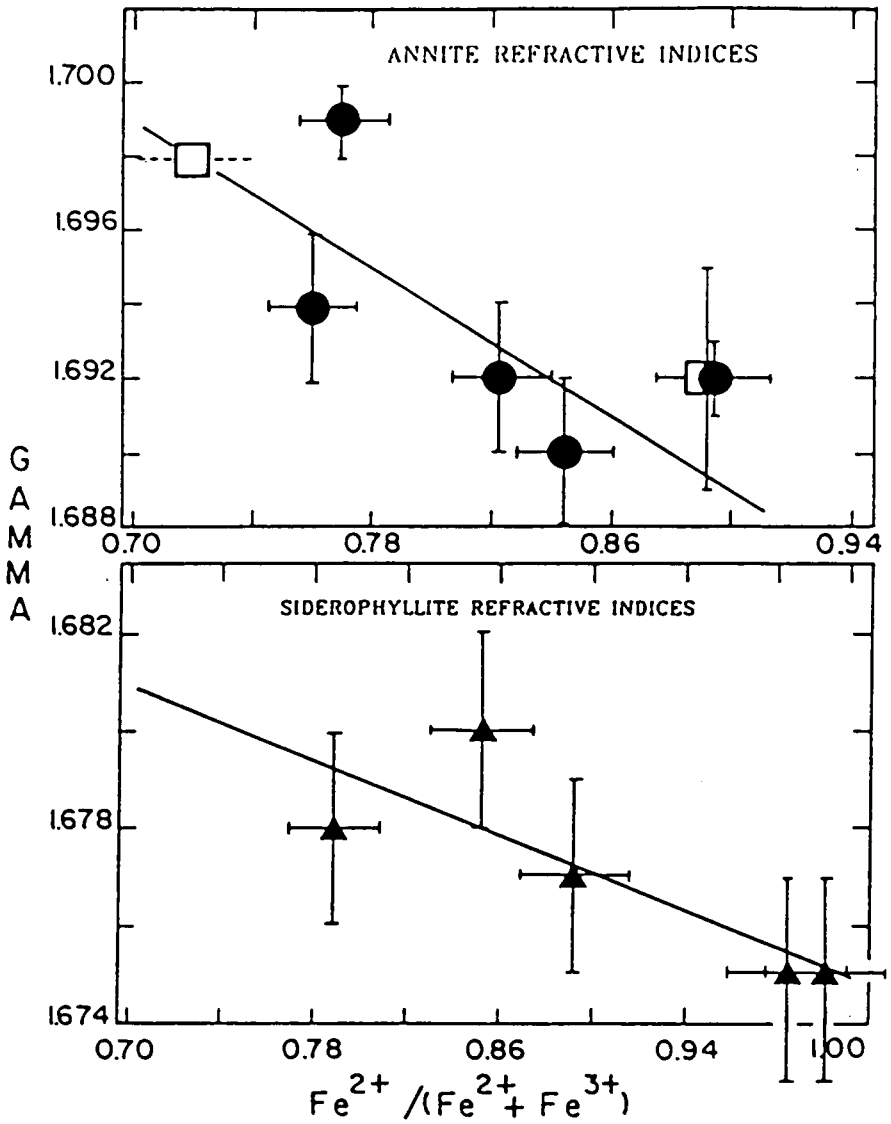

Figure 5. γ-refractive indices versus $Fe^{2+}/ Fe^{2+}+ Fe^{3+}$ ratios ratios for selected synthetic annites and siderophyllites. Errors are ± 0.002 units of the vertical scale and as on previous figures on the horizontal scale.

of Solberg et al (1981). Representative extrapolations of Fe, K, Al and Si for an annite and a siderophyllite are shown in figures 6 and 7. Table 3 gives representative extrapolated probe values for both compositions in this study. Most of the analyses showed that the K content was not always stoichiometric. The general stoichiometry of biotite requires 1 mole of alkali, but chemical analyses of biotites, both natural and synthetic, frequently indicate that alkali contents are low by about 10%. A similar deficiency was observed in most of these synthetic biotites. A few points (< 1%) fell significantly off the extrapolation curve for several samples, giving K values of less than 0.4 wt. % oxide; these most likely represent a K-poor, minor accessory phase.

Within analytical error, the Fe contents of the synthetic biotites were identical with the stoichiometric value for the phase. Both Al and Si were very close to the ideal stoichiometry for most biotites synthesized. An exception was the annite annealed on the FMQ buffer; this run contained many Al-deficient grains, perhaps indicative of a small amount of solid solution with ferri-annite.

Ferrous iron contents were determined using the procedure of Whipple (1974). Samples of 20–25

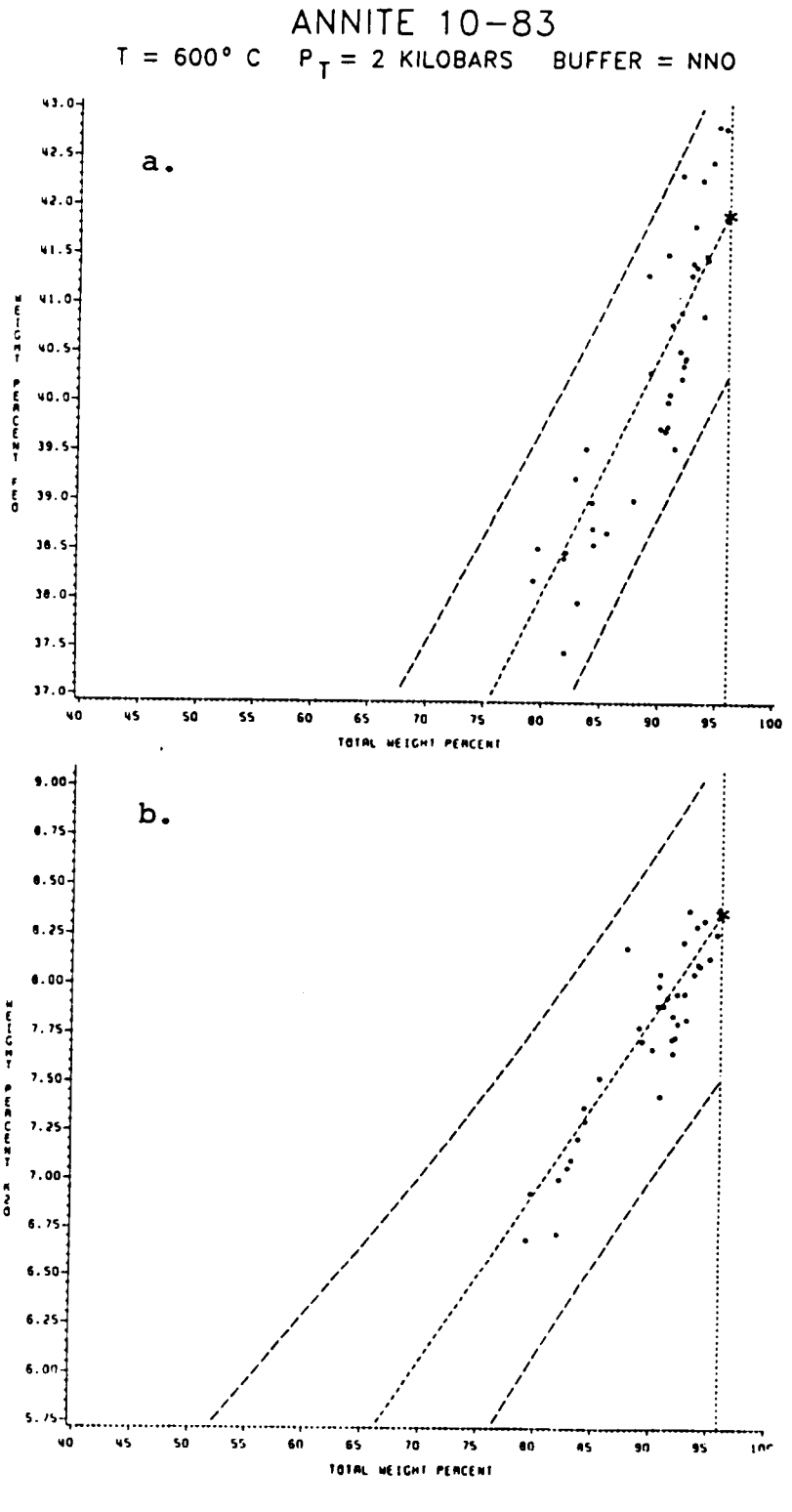

Figure 6a and b. FeO and K_2O as weight percent oxide values for annite 1083 plotted against total analytical sum. These points represent electron microprobe values for individual crystals. The regression line is weighted by the square of the total sum. The line is bracketed by the 95 percent confidence intervals. Values for the oxides are obtained by reading the curve at the ideal 96 wt. % total analytical sum.

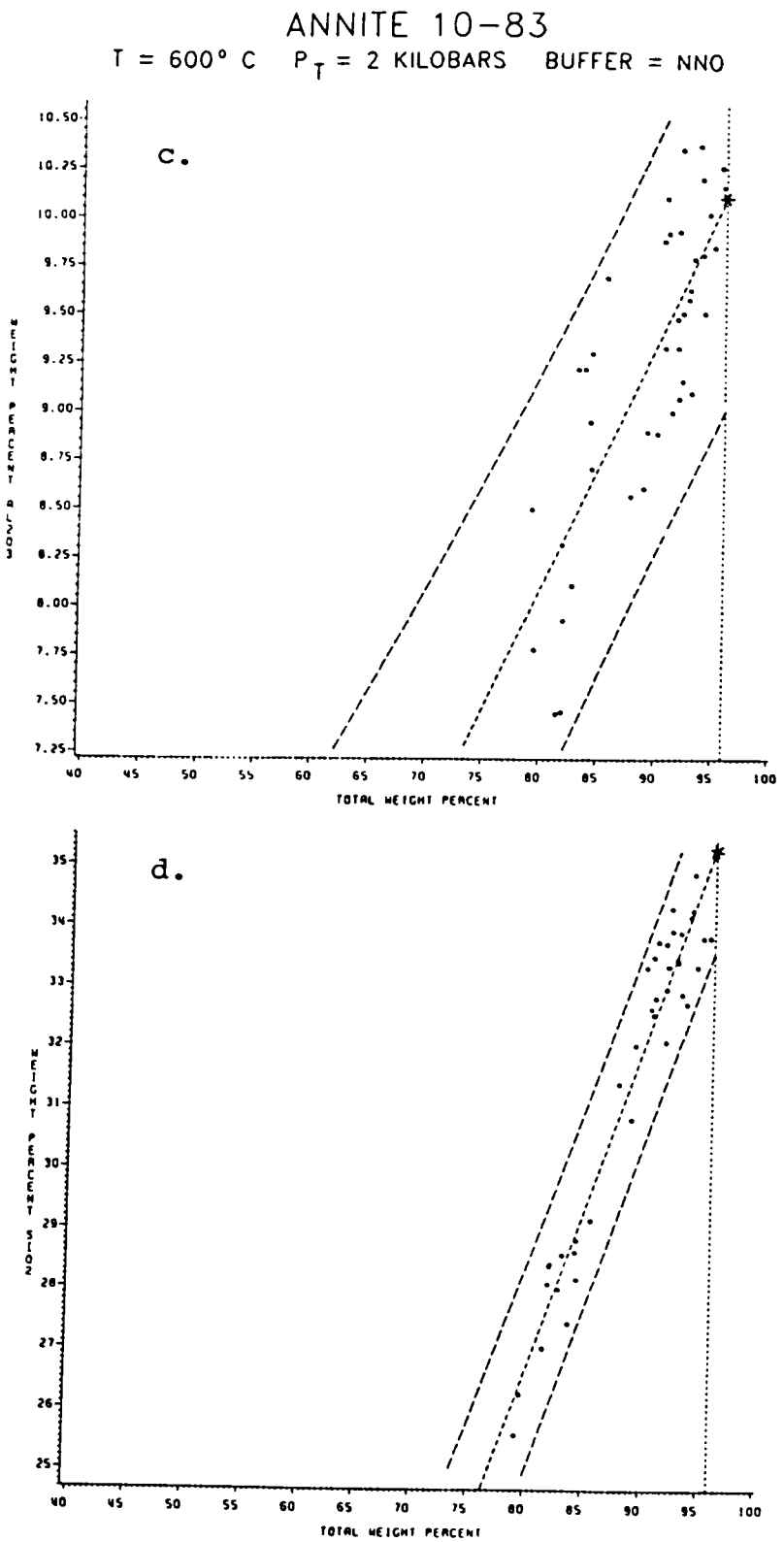

Figure 6c and d. Al_2O_3 and SiO_2 versus total analytical sum for annite 1083.

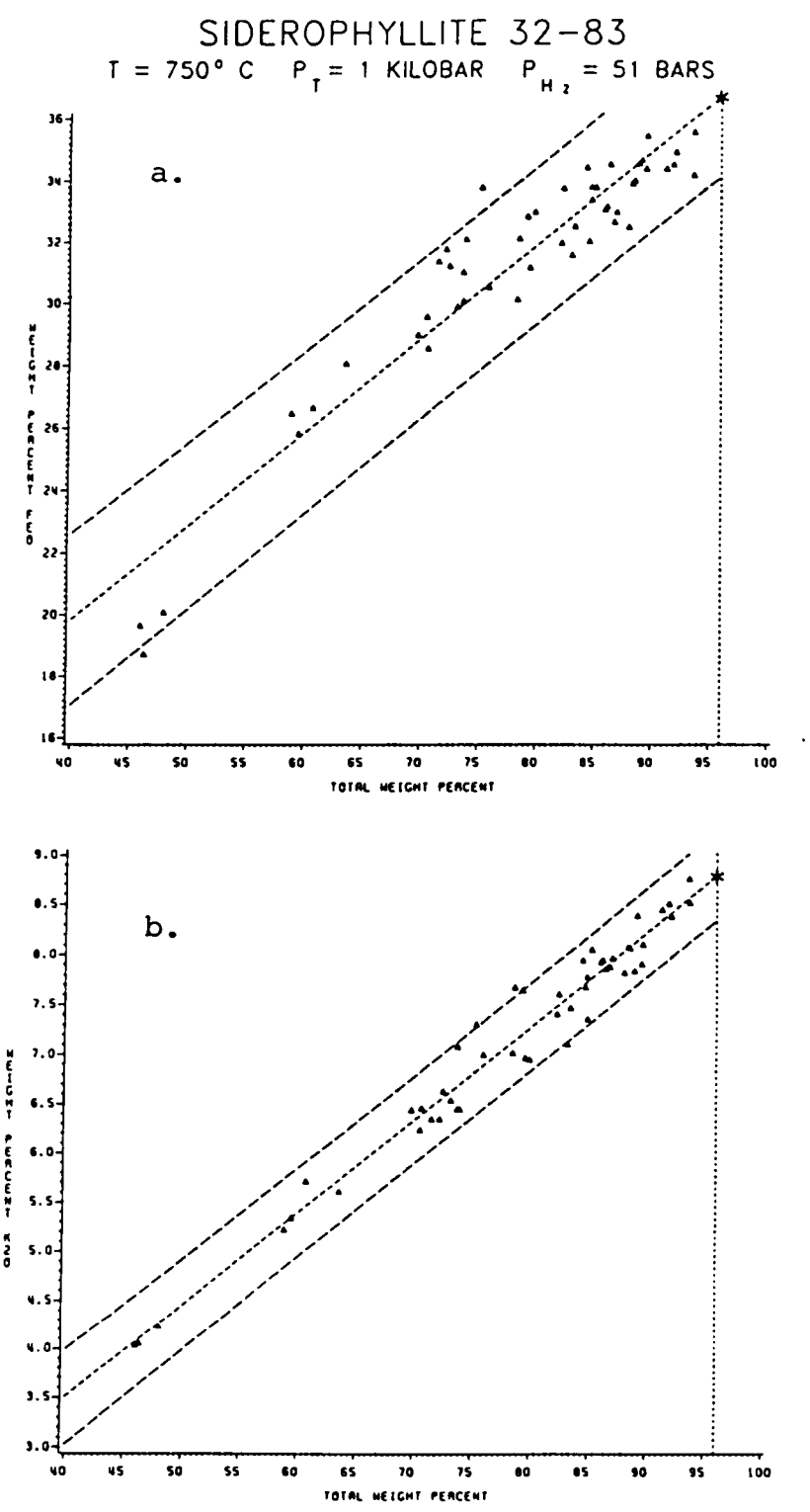

Figure 7a and b. FeO and K_2O versus total analytical sum for siderophyllite 3283. See figure 6 for further explanation.

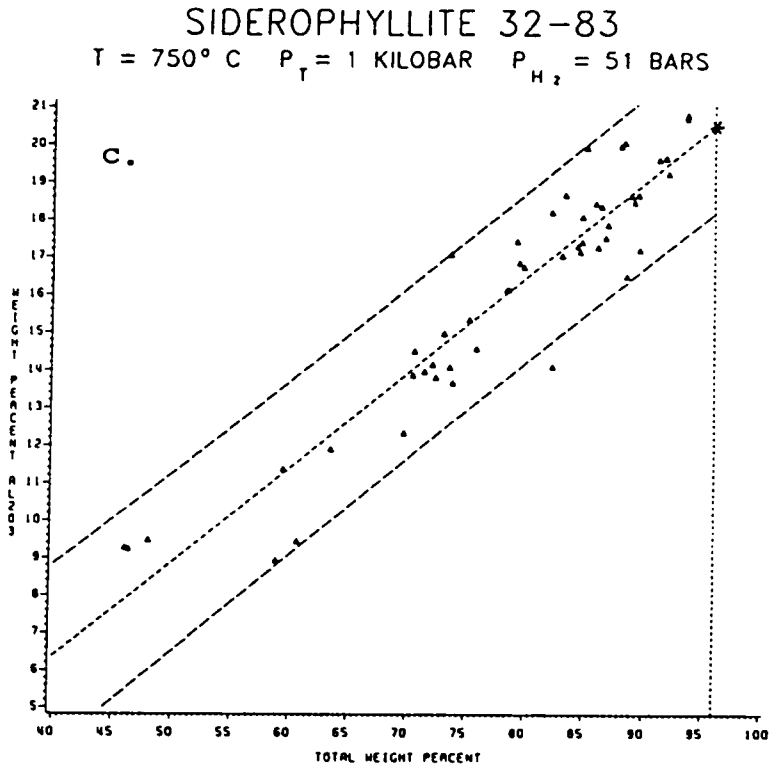

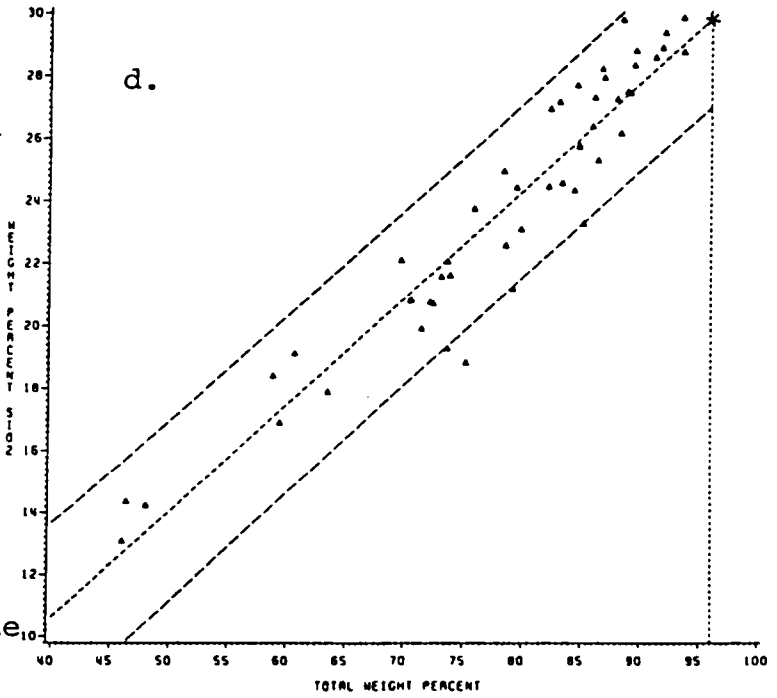

Figure 7c and d. Al_2O_3 and SiO_2 versus total for siderophyllite, 3283.

Table 3. Extrapolated electron microprobe compositions for selected runs, assuming 4.0 wt. % H_2O. See text and figures 6 and 7 for further explanation.

	1083	3183	21a83	7a83	3283
SiO_2	35.30	36.00	30.40	34.00	29.80
Al_2O_3	10.10	20.70	20.20	9.90	20.40
FeO*	41.90	35.70	35.90	43.35	36.60
K_2O	8.35	9.10	8.90	8.39	8.80
total	95.65	96.10	95.40	95.64	95.60
Si	6.03	5.04	5.06	5.88	4.97
Al^{iv}	1.97	2.96	2.94	2.02	3.03
Al^{vi}	0.06	1.07	1.02	0.00	0.98
Fe^{2+}	5.98	4.92	5.00	6.27	5.11
K	1.82	1.91	1.89	1.85	1.87
xii vac	0.18	0.09	0.11	0.15	0.13

OH = 4.0

*Total iron as FeO. Because analytical total Fe was equal to the stoichiometric values for annite (42.19 wt. %) and siderophyllite (35.02 wt. %), within analytical error, the stoichiometric values were used to calculate $Fe^{2+}/ Fe^{2+} + Fe^{3+}$ ratios.

mg of the annealed biotite were dried at 50°C for 18 hours, cooled 30 minutes, and then immediately weighed. A pentavalent vanadium reagent was added prior to dissolution in HF to oxidize the ferrous iron immediately upon release from the biotite. Boric acid was added to complex the fluoride. A ferrous ammonium sulfate reagent, sufficient to reduce all V^{5+} in solution, was added to both blanks and samples. The samples had more ferrous iron in solution than the blanks. The quadrivalent vanadate and ferrous iron were titrated with potassium dichromate, using sodium diphenylamine p-sulfonic acid as an indicator and a 4:4:2 reagent of H_2O, H_2SO_4 and H_3PO_4 to complex the ferric iron and thus adjust the potential of the solution. A reduction of the titre of both blanks and samples with time was observed. This problem was found to be caused by the oxidation over time of the ferrous ammonium sulfate. It was compensated for by constructing a correction curve from data on the natural biotite standard, ORB-44 (which had been used as a control during most analyses). The few annite data points that were affected by this were all corrected to values near those obtained by using fresh Fe^{2+} reagent.

Accuracy of the method was checked by analyzing synthetic fayalite and a natural biotite from the Lucerne pluton, Maine (ORB-44: FeO = 22.74 and Fe_2O_3 = 5.35

wt. %, donated by D. R. Wones). FeO values determined in this study were within 0.3 wt. % of the stoichiometric or previously reported values for these materials.

The data listed in Table 1 were plotted on a log fH_2 versus $Fe^{2+}/Fe^{2+}+Fe^{3+}$ diagram, shown in figure 8. There appear to be two sets of trends; solid curves are drawn for annite and siderophyllite using the data points with the highest run yields. Except for the NNO points, these data were all derived using the Shaw bomb experiments. The curves were back-calculated from the log K equation of figure 9, assuming the arguments presented in the discussion. The dashed lines represent the trends through the biotites annealed on the solid oxygen buffers. The points of intersection for these two sets of curves are near the NNO points for both annite and siderophyllite.

The most reduced annite (100 bars H_2) still contains about 11% Fe^{3+}, but at H_2 pressures below 25-50 bars, annite displays a smooth trend of oxidation with increasing fO_2. Siderophyllite displays a similar trend of iron oxidation as the system becomes more oxidizing. In contrast with annite, siderophyllite can be totally reduced at H_2 pressures of 50 bars or greater; thus, all of the ferric iron in siderophyllite reflects the fO_2 conditions of the environment.

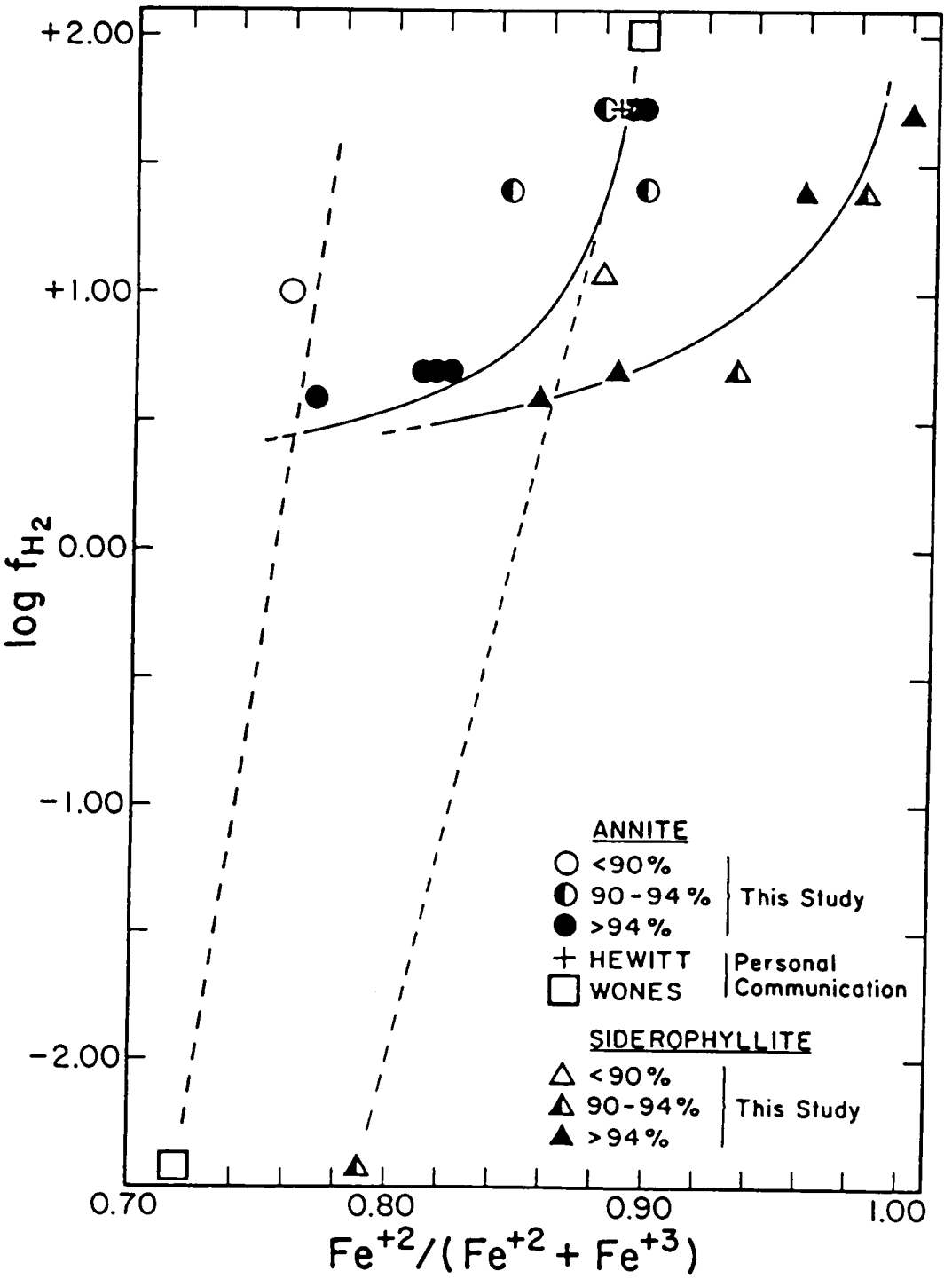

Figure 8. Log fH_2 versus $Fe^{2+}/ Fe^{2+} + Fe^{3+}$ ratios for all runs. Solid curves are back-calculated from the log K curve of figure 9. Dashed curves are fit to the solid buffer runs. See text for further information.

An interesting but distressing outcome of this study is the apparent discrepancy seen between the different methods of annealing. The data in figure 8 show that the runs using solid buffers are not consistent with those using the Shaw membrane. There were no obvious technical difficulties with either method. The hydrogen system did not lose excessive pressure during the run, the membranes appeared to be functioning properly according to the criteria set forth by Hewitt (1977), and the charge was wet in all cases. In every solid-buffered run, both buffer and charge were wet, and the buffer showed both the appropriate oxidized and reduced phases. These points, and the fact that each of the methods was internally consistent, support the argument that the problem is a systematic one. One possible explanation is that the fO_2 values of the solid buffers were not the actual values seen by the biotites. This could occur if the buffering effectiveness of the buffer were exceeded by that of the bomb. Because the bomb buffer is close to NNO (a Rene 41 bomb), one would then expect only the NNO runs to correlate well with the hydrogen runs, and that the FMQ and MH runs would not. A comparison with the Shaw bomb data suggests that the hydrogen fugacities for the FMQ runs were intermediate between the FMQ and the NNO buffers and those for the MH runs were intermediate

between the NNO and MH buffers. It cannot be explained why a technique as demonstrably reliable as the solid oxygen buffers would not work in these experiments, but the trends of the discrepancies suggest this as a possibility. In light of this, only the Shaw bomb data (and the NNO points) will be included in the following discussion.

Discussion

The data in figure 8 indicate that there are two factors affecting the ferric iron content of biotite. The first is indicated by the offset between the annite and siderophyllite curves corresponding to that portion of the Fe^{3+}, required in annite but unnecessary in siderophyllite, needed to articulate the tetrahedral and octahedral sheets. In order to be stable, annite requires that 11% of the octahedral sites be filled by Fe^{3+}, exactly the amount predicted by Hazen and Wones in 1972. The second factor is shown by the shapes of the curves in figure 8. The changing oxidation conditions of the environment require changes in the oxidation state of Fe in both biotites. Changes in Fe^{3+} contents are small for hydrogen fugacities greater than 50 bars. Below that, significant amounts of Fe^{3+} form with decreasing hydrogen fugacity. The similar shapes of the curves

suggest that the oxidation reaction is the same for both compositions.

Siderophyllite is compositionally related to annite by a Tschermak's substitution of $Al^{vi} + Al^{iv}$ for Fe + Si (17% Tschermak's component in siderophyllite). This substitution corrects the misfit between the layers by increasing the size of the tetrahedral layer and decreasing the size of the octahedral layer. Hazen and Wones' (1972) argument for stabilizing the annite structure by a Tschermak's substitution is substantiated in this study by the negligible Fe^{3+} contents in siderophyllite at high H_2 pressures (figure 8). It would be incorrect to assume that one could simply interpolate $Fe^{2+}/Fe^{2+}+ Fe^{3+}$ values for biotites intermediate between annite and siderophyllite. This is shown by calculating the minimum amount of Tschermak's component needed to articulate the octahedral and tetrahedral layers in an ideal annite-siderophyllite solid solution. The calculation is based on the following assumptions:

1) $\underline{b}$ = 9.359 Å for annite, annealed at 50 bars H_2, and containing 11% Fe^{3+} in the octahedral sites (Table 2). Using the Shannon and Prewitt (1970) radii, the calculated b dimension for an octahedral layer with 100% Fe^{2+} is $\underline{b}$ = 9.422 Å;

2) The tetrahedral rotation ($\alpha \cong 0°$) and octahedral

flattening ($\psi \cong 58.3°$) present in annite (Hazen and Burnham, 1973), remain constant;

3) <M-O> values can be calculated from the Shannon and Prewitt (1970) radii;

4) <T-O> values can be calculated from the equation given by Hazen and Burnham (1973).

The calculation predicts that only 10% Tschermak's component is needed to eliminate the steric misfit. Therefore, it is proposed that all Fe-rich biotites containing greater than this critical amount of Tschermak's component will plot on the siderophyllite curve, and will only show significant changes in Fe^{3+} contents as the hydrogen fugacity is decreased below 50 bars. Biotites containing less than 10% Tschermak's component will plot on curves lying between those in figure 8.

The substitution of Mg for Fe has a similar effect in correcting the steric misfit in annite. Using the same set of assumptions, there will be a match between the octahedral and tetrahedral layers at $X_{Mg} \cong 0.24$. As most biotites contain both Al and Mg, it can be predicted that they will plot on or near the same curve as the siderophyllite data (figure 8) when $Al^{vi}/0.3 + Mg/0.72 \geq 1$. If this prediction can be substantiated by further

experimentation, we should be able to construct a useful oxy-thermobarometer based on the Fe^{3+} contents of biotites.

Assuming that the oxidation mechanism is the same for both compositions, it should be possible to combine the data for annite and siderophyllite on a single equilibrium curve. In this treatment, it is assumed that the offset between the annite and siderophyllite curves (figure 8) is due to that portion of the Fe^{3+} in annite required for the fit between the tetrahedral and octahedral layers, and that the changes in Fe^{3+} content in siderophyllite represent only the simple oxidation-reduction reaction. This reaction involves a coupled substitution of up to two moles of Fe^{3+} for every molecule of biotite and applies to both the annite and siderophyllite bulk compositions. The reaction and its associated equilibrium constant are,

$$(3)\quad Fe^{2+}(OH)^- \rightleftarrows Fe^{3+}O^= + 1/2\ H_2$$

$$K_3 = (a_{Fe^{3+}O^=}/a_{Fe^{2+}(OH)^-})fH_2^{\frac{1}{2}}$$

Assuming ideal solution, the equilibrium constant for equation (3) becomes ,

$$K_3 = (X_{Fe^{3+}O^=}/X_{Fe^{2+}(OH)^-})fH_2^{\frac{1}{2}}$$

Remembering that only 2 of the 3 irons in annite and 2 of the 2.5 irons in siderophyllite can be oxidized

by reaction (3) and assuming that reaction (3) accounts for all the non-steric ferric iron, the equilibrium constant can be rewritten as,

$$K_3 = \underset{\text{annite}}{\frac{Fe^{3+}}{Fe^{2+}-1}\, fH_2^{\frac{1}{2}}} = \underset{\text{siderophyllite}}{\frac{Fe^{3+}}{Fe^{2+}-0.5}\, fH_2^{\frac{1}{2}}}$$

At this stage, the equation for annite includes the structurally required Fe^{3+}, and therefore the equations in this form do not plot as the same line on a log K versus 1/T diagram. Correction for the steric effect in annite can be made by subtracting the difference in $Fe^{3+}/Fe^{2+}+Fe^{3+}$ between annite (0.89 ±0.01) and siderophyllite (0.99 ±0.01) at 50 bars P_{H_2} and T = 750° C. Because this Fe^{3+} is due only to the steric effect in annite and is independent of T and fH_2, the resultant equilibrium constant in equation (4) is a function of only the iron involved in the oxidation-reduction reaction.

$$(4)\quad K_3 = \underset{\text{annite}}{\left[\frac{Fe^{3+}}{Fe^{2+}-1} - 0.185\right] fH_2^{\frac{1}{2}}} = \underset{\text{siderophyllite}}{\frac{Fe^{3+}}{Fe^{2+}-0.5}\, fH_2^{\frac{1}{2}}}$$

Figure 9 is a log K_3 versus 1/T plot incorporating all of the data in this study. Error brackets (1σ) are included based on the average

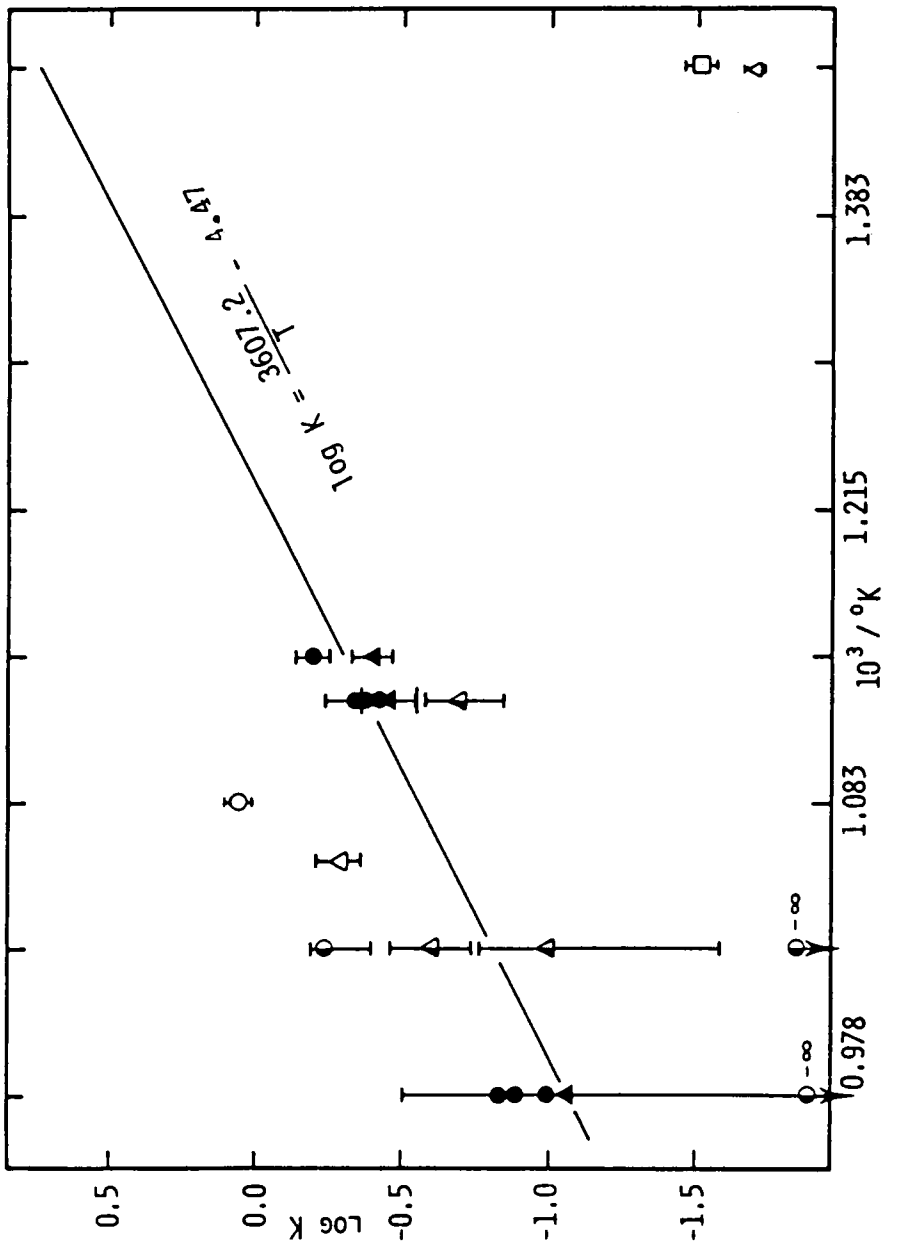

Figure 9. Log K versus $10^3/T$. Symbols are as in figure 8. Error bars represent the total range of uncertainty in the calculated log K values. Those points with overlapping error bars are shown within the same error bar. The regression line was calculated using the high-yield H_2 and NNO runs, using the following equilibrium constant equations for annite and siderophyllite, respectively:

$$K = \left(\frac{Fe^{3+}}{Fe^{2+} - 1} - 0.185\right) f H_2^{\frac{1}{2}} = \left(\frac{Fe^{3+}}{Fe^{2+} - 0.5}\right) f H_2^{\frac{1}{2}}$$

additive errors in the equilibrium constant. Except for the biotites annealed on the FMQ and MH buffers, the data all lie on the line:

$$\log K_3 = 3607.2/ T - 4.47 \quad R^2 = 0.79$$

Even if the FMQ points are disregarded on the basis of poor yield and non-homogeneous composition, there are no obvious explanations for the large discrepancy between the MH data and the rest of the data. If the curve in figure 9 is extrapolated to the conditions of the MH buffer at 400° C, it predicts that the biotites annealed under those conditions should be totally oxidized. However, the titration data indicates only 28% oxidation of the annite and 21% oxidation of the siderophyllite.

Alternatively, if the solid buffer and Shaw buffer data are treated separately, two trends emerge that are equivalent to the intersecting trends in figure 8. As before, the two trends cannot be reconciled without the input of additional data (see Appendix). The predominance of evidence suggests that the Shaw bomb data be preferred.

If the reaction model and equilibrium constant given in equations (3) and (4) are correct, the relation shown in figure 9 should be applicable to a range of biotite compositions. The expression for

the equilibrium constant will change slightly because of differences in the total iron content and because of changes in the structurally required Fe^{3+}. This curve should not be used as presented for the evaluation of thermodynamic properties of biotite. It is a valid way to correllate most of the data in this study, and may be useful as a determinative curve. The set of modified equilibrium constants can be summarized as follows for the Fe-Mg-Al biotites where R is a constant proportional to the structurally required Fe^{3+}:

(5a) $\frac{Al^{vi}}{0.3} + \frac{Mg}{0.72} \geq 1, \quad K_3 = \frac{Fe^{3+}}{Fe^{2+}} f H_2^{\frac{1}{2}}$

$(Al^{vi} + Mg \geq 1)$

(5b) $\frac{Al^{vi}}{0.3} + \frac{Mg}{0.72} \geq 1, \quad K_3 = \frac{Fe^{3+}}{Fe^{2+} - (1-Al^{vi}-Mg)} f H_2^{\frac{1}{2}}$

$(Al^{vi} + Mg < 1)$

(5c) $\frac{Al}{0.3} + \frac{Mg}{0.72} < 1, \quad K_3 = [\frac{Fe^{3+}}{Fe^{2+} - (1-Al^{vi}-Mg)} - 0.185] f H_2^{\frac{1}{2}}$

$(Al + Mg < 1)$

If additional experiments validate the suggestions in this study, the occurrence of Fe-rich biotites in geologic environments can be used as oxy-

thermobarometers requiring only the measurement of the ferric iron content of the biotite. When combined with data from a coexisting phase, such as ilmenite or magnetite, a powerful petrologic indicator may emerge. At this point, many assumptions need to be proven and critical experiments performed, but the potential of the method suggests that future studies will be very rewarding.

References

Appleman, D. E., and H. T. Evans, Job 9214 : Indexing and least-squares refinement of powder diffraction data, U. S. Dept. Commerce, Natl. Tech. Inform. Serv., PB 216 188

Eugster, H. P., 1957, Heterogeneous reactions involving oxidation and reduction at high pressures and temperatures, J. Chem. Phys. v.26, p 1760

___ and D. R. Wones ,1962, Stability relations of the ferruginious biotite, annite, J. Pet. v.3, pt.1, pp 82-125

Ferry, J.M., and F.S. Spear, 1978, Experimental calibration of the partitioning of Fe and Mg between biotite and garnet, Contrib. Mineral. Petrol. v.66, pp 113-117

Guidotti, C. V., J. T. Cheney, and P. D. Conatore, 1975, Interrelationship between Mg/Fe ratio and octahedral Al content in biotite, Am. Min. v.60, pp 849-853

Hazen, R.M., and C.W. Burnham, 1973, The crystal structures of one-layer phlogopite and annite, Am. Min. v.58, pp 889-900

___ and D. R. Wones, 1972, The effect of cation substitutions on the physical properties of trioctahedral micas, Am. Min. v.57, pp 103-125

___ and D.R. Wones, 1978, Predicted and observed compositional limits of trioctahedral micas, Am. Min. v.63, pp 885-892

Hewitt, D. A., 1977, Hydrogen fugacities in Shaw bomb experiments, Contr. Mineral. Petrol. v.65, pp 165-169

___ 1978, A redetermination of the fayalite-magnetite-quartz equilibrium between 650° C and 850° C, Am. J. Sci. v.278, pp 715-724

___ and D. R. Wones, 1975, Physical properties of some synthetic Fe-Mg-Al trioctahedral biotites, Am. Min. v.60, pp 854-862

___ and D.R. Wones, 1981, The annite-sanidine-magnetite equilibrium, G.A.C./M.A.C./C.G.U. Abstracts, v.6

Holdaway, M.J., and S.M. Lee, 1977, Fe-Mg cordierite stability in highgrade pelitic rocks based of experimental, theoretical, and natural observations, Contrib. Mineral. Petrol. v.63, pp 175-193

Huebner, J.S., and M. Sato, 1970, The oxygen fugacity-temperature relationships of manganese oxide and nickel oxide buffers, Am. Min., v.55, pp 934-952

Munoz, J.L., and S.D. Ludington, 1974, Fluoride-hydroxyl exchange in biotite, Am. J. Sci. v.274, pp 396-413

Myers, J. and H.P. Eugster, 1983, The system Fe-Si-O: Oxygen buffer calibrations to 1,500 K, Contr. Mineral. Petrol. v.82, pp 75-90

Rutherford, M.J., 1969, An experimental determination of iron biotite-alkali feldspar equilibria, J. Pet. v.10, pt. 3, pp 381-408

___ 1973, The phase relations of aluminous iron biotites in the system $KAlSi_3O_8$-$KAlSiO_4$-Al_2O_3-Fe-O-OH, J. Pet. v.14, pt. 1, pp 159-180

Schairer, J. F. and N. L. Bowen, 1955, The system K_2O-Al_2O_3-SiO_2 Am. J. Sci. v.253, pp 681-746

Shannon, R.D., and C.D. Prewitt, 1970, Revised values of effective ionic radii, Acta Cryst., B26, pp 1046-1048

Shaw, H.R., 1967, Hydrogen osmosis in hydrothermal experiments, Abelson, P.H., ed., Researches in Geochemistry v.2, pp 521-541, John Wiley and Sons, N. Y.

Solberg, T.N., J. Abrecht, and D.A. Hewitt, 1981, Graphical procedures for the refinement of electron microprobe analysis of fine-grained particles, Geiss, R.H., ed., Microbeam Analysis, San Fransisco Press, Inc.

Tuttle, O. F., 1949, Two pressure vessels for silicate-water studies, Geol. Soc. America Bull. v.60, pp 1727-1729

Whipple, E.R., 1974, A study of Wilson's determination of ferrous iron in silicates, Chem. Geol. v.14, pp 223-238

Wones, D.R., R.G. Burns and B.M. Caroll, 1971, Stability and properties of synthetic annite (abstr), Am. Geophys. Union v.52, pp 369-370

___ and H.P. Eugster, 1965, Stability of biotite; Experiment, theory, and application, Am. Min. v.50, pp 1228-1273

APPENDIX

Additional experimental studies needed on the ferric iron content of biotite:

1) H_2 and/or H_2O analyses should be run on all samples to determine if H_2 content changes proportionally with Fe oxidation.
2) Duplicate experiments using the solid oxygen buffers should be run, especially for MH, carefully monitoring the system for equilibrium.
3) Multiple runs should be made using the Shaw technique, keeping the H_2 pressure constant and varying the temperatures.
4) Biotites between annite and siderophyllite in Al-content should be synthesized and ferric/ferrous ratios obtained.
5) The experimental system needs to be extended from the Fe-Al system to the Fe-Al-Mg system.

The vita has been removed from the scanned document